

Extracellular Matrix Density Regulates Extracellular Proteolysis via Modulation of Cellular Contractility

Alakesh Das, Aastha Kapoor, Gunjan D Mehta, Santanu K Ghosh and Shamik Sen*

WRCBB, Department of Biosciences & Bioengineering, IIT Bombay, India

Abstract

The Extracellular Matrix (ECM) undergoes changes in composition and organization during tumor progression. In breast cancer, increased deposition and cross linking-induced alignment of collagen I create a stiffer microenvironment that directly contributes to cancer invasion. While ECM stiffness-induced invasion has been documented, it remains unclear if ECM density also contributes to invasion independent of ECM stiffness. In this paper, using collagen I-coated glass coverslips of varying density, we sought to study the influence of ECM density on the invasiveness of human MDA-MB-231 breast cancer cells. We first showed that cell spreading and contractility increases with ECM density. Concomitant with increase in cell contractility, matrix degradation was seen to increase with ECM density and was associated with higher invadopodia activity. The density-dependent increase in degradation was associated with higher activity of MMP-2, MMP-9 and MT1-MMP. Treatment with either the MMP inhibitor GM6001 or the myosin II inhibitor blebbistatin, were found to inhibit cell contractility and suppress matrix degradation. Contractility was found to modulate the activity of MMP-2 and MMP-9, and the localization of MT1-MMP at invadopodia. Taken together, our results indicate that ECM density regulates ECM degradation through modulation of cell contractility.

Keywords: Extracellular matrix (ECM); Ligand density, Degradation; Invadopodia; MMP; Contractility; Deadhesion

Introduction

The initial events of cancer metastasis involve degradation of the basement membrane (BM), navigation through the stroma, and entry into the blood vasculature. The abovementioned steps require cancer cells to interact with extracellular matrices (ECM) of varying composition and organization. While the BM is enriched in collagen IV and laminin [1], the tumor stroma is composed of a collagen I-rich network that undergoes reorganization from a random network to a more aligned network as cancer progresses [2,3]. Further, fiber alignment induced by enhanced crosslinking of collagen by lysyl oxidases (LOX) causes ECM stiffening, and has been implicated in cancer progression [4].

Several studies have focused on understanding the influence of ECM composition, ECM density and ECM physical properties on various cellular processes. For example, spreading and motility of NIH 3T3 fibroblasts and smooth muscle cells have been found to exhibit a biphasic response to ECM density [5-7]. In contrast, spreading and cell generated traction forces in breast, lung and prostate cancer cells were found to increase with increasing ECM density [8], highlighting differences in spreading responses between normal and cancer cells. Of the several biophysical characteristics of the microenvironment, ECM stiffness, topography and dimensionality have received a lot of attention. First, studies have established a strong link between ECM stiffness and the invasiveness of cancer cells. In two-dimensional cultures, ECM stiffness has been shown to increase cell proliferation and motility in glioma cells [9]. In mammary epithelial cells, ECM stiffness alone has been shown to be capable of disrupting tissue homeostasis and inducing cancer cell invasion [10]. Using patterning, Doyle et al. demonstrated the similarity of fibroblast migration in 3D fibrillar matrices to migration on one-dimensional lines [11]. Similarly, MDA-MB-231 breast cancer cells were found to migrate far more efficiently on patterned microtracks of collagen I in comparison to 3D collagen matrices [12]. Together, these findings demonstrate the multiple ways in which ECM physical cues regulate cell behavior.

Invadopodia are actin-rich structures that are associated with

ECM degradation and have been implicated in cancer invasion and metastasis [13-16]. When cancer cells are cultured on top of a layer of ECM protein, invadopodia are manifested as small actin dots that protrude into their underlying matrix and cause localized degradation [17]. Several actin regulatory proteins like cortactin and WASP, actin crosslinking proteins like fascin and α -actinin, regulate the formation and dynamics of invadopodia. In addition, adhesion signaling proteins including integrins, FAK and paxillin also localize at invadopodia. Several enzymes including Matrix Metalloproteases (MMPs), ADAMs and seprases, mediate matrix degradation at invadopodia. While formation of invadopodia is actin-dependent, invadopodia growth requires both microtubules and intermediate filament proteins [18].

Several recent studies have highlighted the importance of ECM physical properties on invadopodia formation and dynamics. Using polyacrylamide hydrogels of two different stiffnesses, Weaver and coworkers demonstrated for the first time that ECM rigidity promoted the activity of invadopodia in CA1d breast cancer cells [19]. Moreover, myosin disrupting drugs blebbistatin, Y-27632 and ML7 were all found to inhibit the active degradation at invadopodia in a dose-dependent manner, though the invadopodia structure remained intact. Extending their studies over a wide range of stiffnesses that spanned the kPa-GPa range, they found that ECM degradation exhibited a two-peaked distribution of invadopodia formation with peaks at 30 kPa and 1.8 GPa, respectively [20]. Work from the same group also demonstrated that matrix crosslinking suppresses invadopodia-based degradation [21]. Collectively, these results highlight the strong influence of ECM

*Corresponding author: Shamik Sen, WRCBB, Department of Biosciences & Bioengineering, IIT Bombay, Mumbai 400 076, India, E-mail: shamiks@iitb.ac.in

Received April 26, 2013; Accepted May 30, 2013; Published June 15, 2013

Citation: Das A, Kapoor A, Mehta GD, Ghosh SK, Sen S (2013) Extracellular Matrix Density Regulates Extracellular Proteolysis via Modulation of Cellular Contractility. J Carcinogene Mutagene S13: 003. doi:10.4172/2157-2518.S13-003

Copyright: © 2013 Das A, et al. This is an open-access article distributed under the terms of the Creative Commons Attribution License, which permits unrestricted use, distribution, and reproduction in any medium, provided the original author and source are credited.

mechanical properties on invadopodia formation, dynamics and activity.

While ECM density and ECM stiffness can be independently controlled under *in vitro* conditions, *in vivo*, stiffening of the tumor microenvironment is made possible through increased deposition and crosslinking of collagen I, a process where both ECM density and ECM stiffness are altered. Under these conditions, it is difficult to evaluate the individual contribution of these two factors. In this paper, we have studied the influence of ECM density on the degradation characteristics of MDA-MB-231 human breast cancer cells. On collagen I-coated glass coverslips of varying density, cells were found to spread more and assemble more focal adhesions on higher density surfaces. In line with the density-dependent spreading response, cells were more contractile on higher density surfaces when probed with the trypsin de-adhesion assay. Strikingly, ECM degradation mediated by invadopodia, was also sensitive to ECM density and maximum on the highest density surface. Incubation with the broad-spectrum MMP inhibitor GM6001 or the myosin inhibitor blebbistatin even at low doses reduced cell contractility and suppressed degradation and invadopodia formation. Degradation was found to be mediated by MMP-2, MMP-9 and MT1-MMP in a contractility-dependent manner. Taken together, our results demonstrate the direct influence of ECM density on invasiveness, and highlight the intimate relationship between cell adhesion, cell contractility and ECM proteolysis.

Materials and Methods

ECM coating and quantification

Coverslips were acid washed and sterilized with 70% ethanol for 30 minutes before coating. Glass coverslips were incubated with rat-tail collagen I (Sigma) at theoretical densities of 0.1, 1, 10 $\mu\text{g}/\text{cm}^2$ at 4°C overnight. The following day, after repeated washing, the coverslips were blocked with 2% F127 Pluronic (Sigma) for 10 min at room temperature, and UV sterilized before plating cells. For quantification of ECM coating, samples were stained with collagen I antibody (Bangalore Genei), and imaged at 10x magnification at five random locations under identical camera exposure and gain settings. Analysis of images was done using Image J (NIH) software. The experiment was repeated twice.

Cell culture

MDA-MB-231 cells were obtained from NCCS (National Centre for Cell Science) and cultured in CO₂ incubator (Thermo Scientific) containing 5% CO₂, 95% humidified air and temperature set at 37°C. Cells were grown in DMEM (Dulbecco's Modified Eagle Medium) (Gibco) supplemented with 10% FBS (Gibco) and 1% Penicillin/Amphotericin/Streptomycin antibiotics (Himedia). Cultures were maintained in 25 cm² culture flask (Corning) and passaged when 80% confluent with 0.25% trypsin EDTA (Hi-media).

Immunocytochemistry (ICC)

For staining, cells were first treated with permeabilization buffer for 3 minutes (10mM HEPES, pH 6.9, 50mM NaCl, 3mM MgCl₂, 0.5% Triton X-100, 300mM sucrose, 1mM EGTA, and protease inhibitor cocktail (Sigma)) to wash out cytoplasmic content and then fixed with 4% paraformaldehyde (PFA) (Sigma). After blocking with 2% BSA for one hour at room temperature, cells were incubated with one or more of the following primary antibodies (Ab) overnight in the refrigerator at 4°C: anti-cortactin mouse monoclonal Ab. (1:100, Santa-Cruz), anti-vinculin mouse monoclonal Ab. (1:200, Sigma), anti-MT1-MMP rabbit

monoclonal Ab. (1:200, Abcam), anti-collagen I rabbit polyclonal Ab. (Merck). After washing with 1X PBS twice, cells were incubated for one hour at room temperature (RT) with the following secondary antibodies: Alexa Fluor 488 goat anti-mouse IgG (1:300, Invitrogen), Alexa Fluor 488 anti-rabbit IgG (1:400, Invitrogen), Alexa Fluor 555 donkey anti rabbit IgG (1: 400, Invitrogen). F-actin was stained with Alexa Fluor 488 and Alexa Fluor 555 conjugated phalloidin in 1:300 to 1:400 dilutions for one hour at RT. Dapi (4, 6- diamidino-2-phenylindole, Sigma) was used to stain nucleus at 1:300 dilution.

Microscopy

Most of the experiments were performed using an Olympus IX71 microscope. Images were acquired with a CCD camera (QImaging) using the acquisition software (Image-Pro Express 6.3). For analysis of ECM density-dependent cell spreading, cells were imaged at 10x magnification in phase contrast microscopy, and 50 cells were analyzed per condition across two experiments. Identification of invadopodia formation was based on the co-localization of F-actin/cortactin and cortactin/MT1-MMP, and were acquired using a Zeiss Axio Observer. Z1 microscope (40X Plan-Neofluar objective, NA = 0.75; Carl Zeiss MicroImaging Inc.) equipped with AxioCam camera controlled by Axiovision software (Axio Vision Release 4.8.3 SP1 (06-2012)). Images were processed using the Axiovision software for brightness and contrast adjustment and for merging of the images. For both the measurements, at least 100 cells were analyzed per condition across two independent experiments.

Quantification of focal adhesion size

To determine the distribution of focal adhesions, cells were first treated with permeabilization buffer to remove cytoplasmic content, fixed, and then stained for the focal adhesion protein vinculin. Images were acquired at 40x magnification under identical exposure and gain settings, and then processed in Image J (NIH) using a sequence of image-processing steps, as described elsewhere [22]. Briefly, after background subtraction, images were converted to 8 bit images and then thresholded to the same extent. Thresholded images were then inverted and then quantified for determine the sizes of individual focal adhesions. By repeating these steps for all the conditions (60 cells/condition pooled from two sets of experiments), the mean size of focal adhesions was determined.

Quantification of ECM degradation

To determine density-dependent collagen degradation, 5×10^3 MDA-MB-231 cancer cells were plated on 12 mm collagen-coated glass coverslips and incubated for 24 hrs. Cells were then fixed with 4 % PFA and stained with Alexa Fluor 488 phalloidin for visualizing the F-actin network and DAPI for labeling the nucleus. Further, samples were stained with collagen I antibody to identify patches of degradation. Samples were imaged at 20x magnification in fluorescence microscopy, and at least 100 cells were analyzed per condition across two experiments. The extent of degradation was quantified by first thresholding the raw collagen images using Image J (NIH) and then normalizing the area degraded by each cell by the cell spread area determined from the F-actin staining [23,24].

Gelatin zymography

For zymographic studies, 5×10^4 cells were plated on 18 mm collagen-coated glass coverslips and incubated for 24 hrs. The media was collected and centrifuged at 2000 rpm for 30 min to remove dead cells and any other debris, and supernatants were lyophilized for

zymographic experiments, as described elsewhere [25]. In case of drug studies, cells were allowed to adhere to the substrate for 4 hours, after which fresh media containing drug at desired concentration was added.

Trypsin de-adhesion assay

For preparation of de-adhesion experiments, cells were cultured in collagen-coated petri dishes for 24 hrs. For experiments, petri dishes were placed on the microscope stage, media was discarded, cells were washed with 1X PBS twice and then warm trypsin was added (37°C). Images were acquired with an inverted microscope (Olympus IX71) at 3 sec intervals at 10X magnification, until cells become rounded but remained attached to the substrate. For quantification, cell spread area was measured using Image J (polygonal selection tool). Normalized time dependent de-adhesion dynamics was plotted by dividing the change in cell spreading area at time 't' ($A_{initial} - A(t)$) and the net change in area ($A_{initial} - A_{final}$). Normalized area vs time data was fitted to sigmoidal curve in Origin (Origin Lab) to yield time constants τ_1 and τ_2 , respectively. Statistics were obtained for a total of 30 cells/condition pooled from two sets of experiments.

Results

Quantification of collagen surface adsorption

To study the effect of ECM density on invasive properties of breast cancer cells, glass coverslips were coated with collagen I at the theoretical coating densities of 0.1, 1 and 10 $\mu\text{g}/\text{cm}^2$, respectively, and subsequently blocked with pluronic to minimize any non-specific adsorption of serum proteins. To test the degrees of collagen surface adsorption across the three conditions, coverslips were stained with collagen antibody and imaged (Figure 1A). Quantitative analysis of surface fluorescence at random locations allowed us to assess the amount of surface coating. As observed from the histograms in Figure 1B, right shift in the peak intensity was observed with increase in coating density. Comparison of mean intensities revealed a 50% increase in fluorescence from 0.1 to 1 $\mu\text{g}/\text{cm}^2$, and a further 70% increase from 1 to 10 $\mu\text{g}/\text{cm}^2$ (Figure 1C). Collectively, these results indicated that the three densities chosen were well separated and therefore suitable for studying density-dependent effects.

Influence of collagen density on spreading, cytoarchitecture and focal adhesion organization in MDA-MB-231 breast cancer cells

Cancer progression is associated with increased deposition of collagen I and linearization of collagen fibers mediated by cross linking proteins like Lysyl Oxidase (LOX) [26]. To study the effect of ligand density on spreading area of the highly invasive MDA-MB-231 breast cancer cells, cells were cultured for 24 hrs on the different collagen-coated coverslips. Phase contrast images were acquired at 10X magnification for analysis of the spreading area across the different ligand densities (Figure 2A). On pluronic-coated surfaces which served as negative controls, cell spreading was significantly less compared to spreading on the lowest 0.1 $\mu\text{g}/\text{cm}^2$ collagen-coated surface (Figure 2B), indicating that at the 24 hour time point, passive adsorption of serum proteins was negligible and the effects were purely mediated by the collagen-coated substrates. Comparison of spreading area across the various surfaces revealed an ECM density-dependent response, with maximal spreading observed at the coating density of 10 $\mu\text{g}/\text{cm}^2$. However, no statistical differences were observed between the 1 $\mu\text{g}/\text{cm}^2$ and 10 $\mu\text{g}/\text{cm}^2$ surfaces, indicating a saturation response on surfaces coated with collagen at densities of 1 $\mu\text{g}/\text{cm}^2$ and beyond.

To further probe if the increased spreading on higher density surfaces was associated with alterations in the cell cytoskeleton and the organization of focal adhesions, cells were stained for F-actin and vinculin, respectively (Figure 2C). While prominent stress fibers were observed across all conditions, differences were observed in the number and size distribution of focal adhesions, as visualized with the prominent focal adhesion protein vinculin. Quantitative image analysis revealed a statistically significant increase in the size of focal adhesions observed on the 1 $\mu\text{g}/\text{cm}^2$ and 10 $\mu\text{g}/\text{cm}^2$ surfaces in comparison to the 0.1 $\mu\text{g}/\text{cm}^2$ collagen-coated surface (Figure 2D). Collectively, these results indicate that increase in ECM density is associated with increase in cell spreading mediated by formation of stronger focal adhesions.

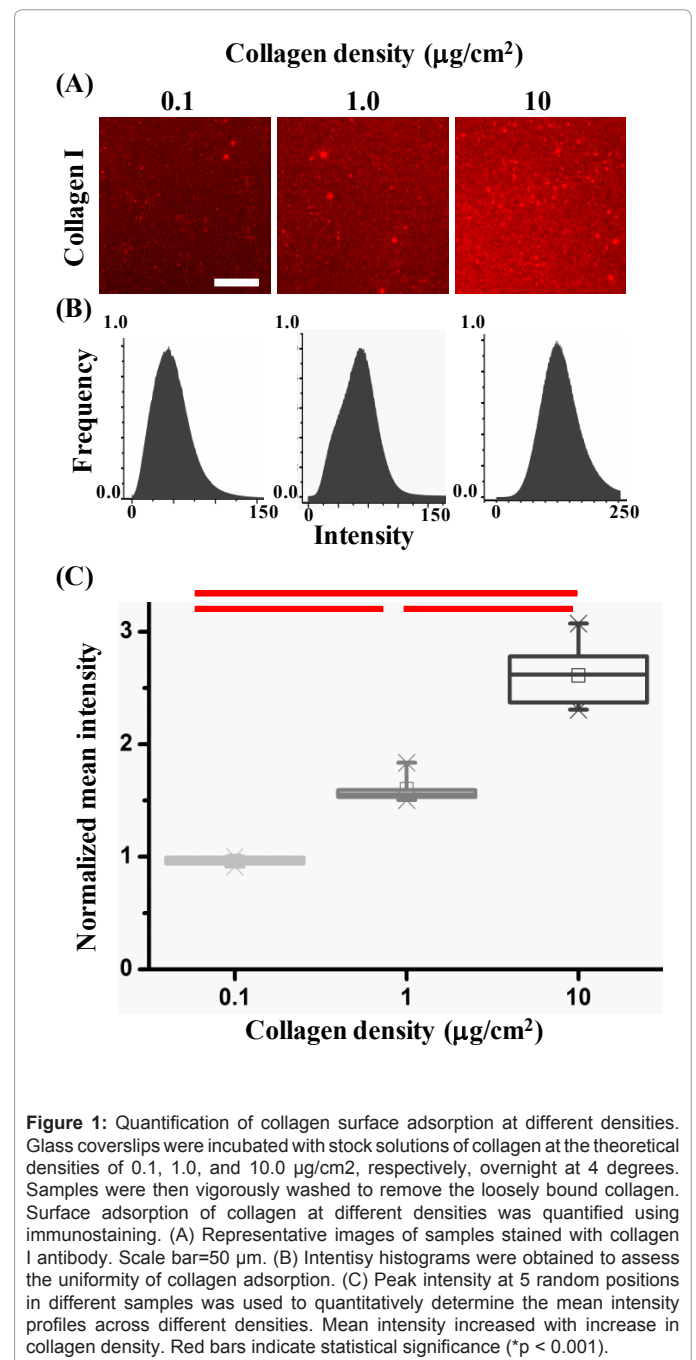


Figure 1: Quantification of collagen surface adsorption at different densities. Glass coverslips were incubated with stock solutions of collagen at the theoretical densities of 0.1, 1.0, and 10.0 $\mu\text{g}/\text{cm}^2$, respectively, overnight at 4 degrees. Samples were then vigorously washed to remove the loosely bound collagen. Surface adsorption of collagen at different densities was quantified using immunostaining. (A) Representative images of samples stained with collagen I antibody. Scale bar=50 μm . (B) Intensity histograms were obtained to assess the uniformity of collagen adsorption. (C) Peak intensity at 5 random positions in different samples was used to quantitatively determine the mean intensity profiles across different densities. Mean intensity increased with increase in collagen density. Red bars indicate statistical significance (* $p < 0.001$).

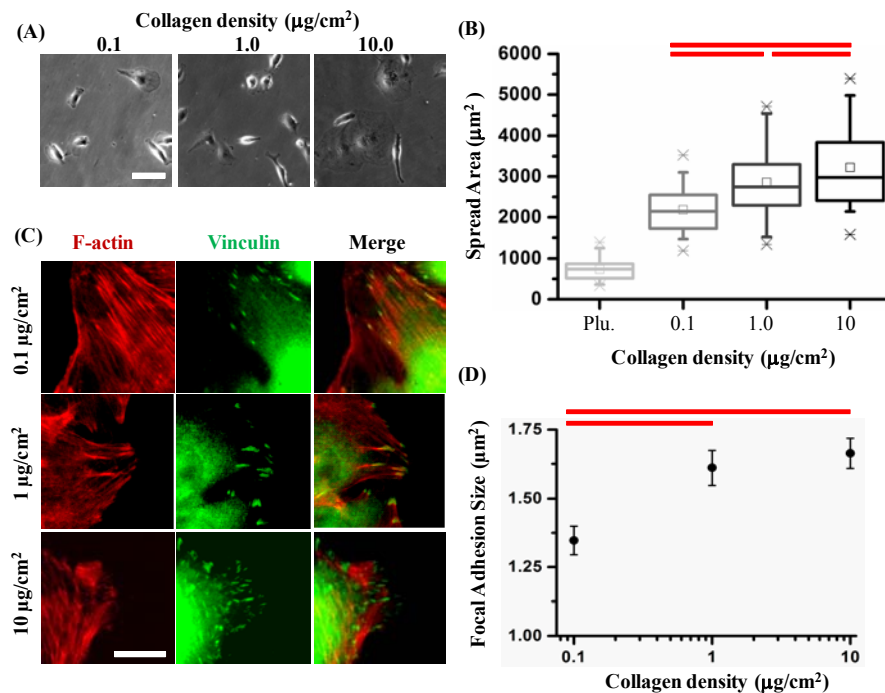


Figure 2: Influence of collagen density on spreading, cytoarchitecture and focal adhesions in MDA-MB-231 cells. (A) Representative phase contrast images of MDA-MB-231 cells cultured on collagen-coated coverslips at different densities for 24 hours. Scale bar=50 µm. (B) Projected cell area on coverslips coated with collagen at varying densities. Pluronic-blocked coverslips (Plu.) without any matrix coating served as negative controls. Cell spreading increased with increasing ECM density. Bars indicate statistical significance (*p < 0.05). (C) F-actin (red) and vinculin (green) distribution in cells cultured on collagen-coated surfaces at varying densities. Merged images show the co-localization of the actin fibers and vinculin at the points of focal adhesion formation (yellow). Prominent stress fibers were observed across all the conditions. Scale bar=20 µm. (D) Average size of focal adhesions increased with increasing collagen density. Bars indicate statistical significance (*p < 0.001).

Influence of collagen density on cellular contractility

The above studies clearly demonstrated that increase in ligand density leads to stronger adhesions. Given the close crosstalk between adhesion maturation and cell contractility, we hypothesized that increase in ligand density would enhance cell contractility. We tested this directly using the trypsin de-adhesion assay, where contractility is indirectly measured by tracking the retraction kinetics of cells upon incubation with trypsin [27]. Briefly, cells were washed with PBS, incubated with warm trypsin, and images acquired at 5 sec intervals until cells became rounded but remained attached to the substrate. As seen from representative detachment responses of cells cultured on various collagen-coated substrates, while faster cell rounding was observed on the higher density surfaces (Figure 3A), detachment responses across all the three conditions were sigmoidal in nature (Figure 3B), as observed with other adherent cell types. Fitting the normalized de-adhesion curves with Boltzmann equation allowed us to obtain the time constants τ_1 and τ_2 and assess their alterations across the different conditions. Increase in ligand density was associated with a nearly 40% reduction in τ_1 from ~100 s on 0.1 µg/cm² surfaces to ~60 s on 10 µg/cm² surfaces (Figure 3C). Similarly, τ_2 values decreased from ~30 s on 0.1 µg/cm² surfaces to ~20 s on 10 µg/cm² surfaces representing a ~70% drop (Figure 3D). Since faster de-adhesion is associated with increased contractility, these results demonstrate that increase in collagen density is associated with increased cellular contractility.

Influence of collagen density on degradation characteristics of MDA-MB-231 cells

Cancer cells are known to modulate their underlying ECM through

a combination of protease-mediated degradation using various proteases like MMPs (MMP-2, MMP-9, MT1-MMP, etc) [28] and force-driven remodeling. While our de-adhesion results indicate an upregulation of cell tractions with increase in ECM density, the extent of degradation on the various matrices remained unclear. To determine this, equal number of cells were placed on surfaces of varying collagen concentration, and samples were immunostained with collagen I antibody to visualize the degradation pattern (Figure 4A), phalloidin (green) to visualize the cell periphery and DAPI (blue) to mark the cell nucleus. Interestingly, quantitative analysis of the degraded areas across the different density surfaces revealed an increase in degradation area with increase in ligand density (Figure 4B). In comparison to the lowest density surface, degradation was ~2 fold higher on the 1 µg/cm² surfaces and ~4 fold higher on the 10 µg/cm² surfaces. Together, these data indicate that matrix degradation increases with ECM density. Similar density dependent degradation was also observed on gelatin-coated and fibronectin-coated substrates (Figures S1 and S2).

Influence of collagen density on invadopodia formation

While the above results clearly demonstrated enhanced degradation on denser substrates, the mode of degradation was not clear from the low magnification images. To probe this further, cells were imaged at higher magnification to detect the formation of invadopodia, actin-rich invasive structures formed on the ventral surface of the cells in contact with the underlying matrix [29,30]. Invadopodia formation was assessed at the 24 hour time point by co-staining cells with invadopodia markers actin and cortactin, and manual counting of sites of co-localization of the two markers (Figure 5A). Comparative analysis of invadopodia per cell across varying density of ligands revealed that cells on higher

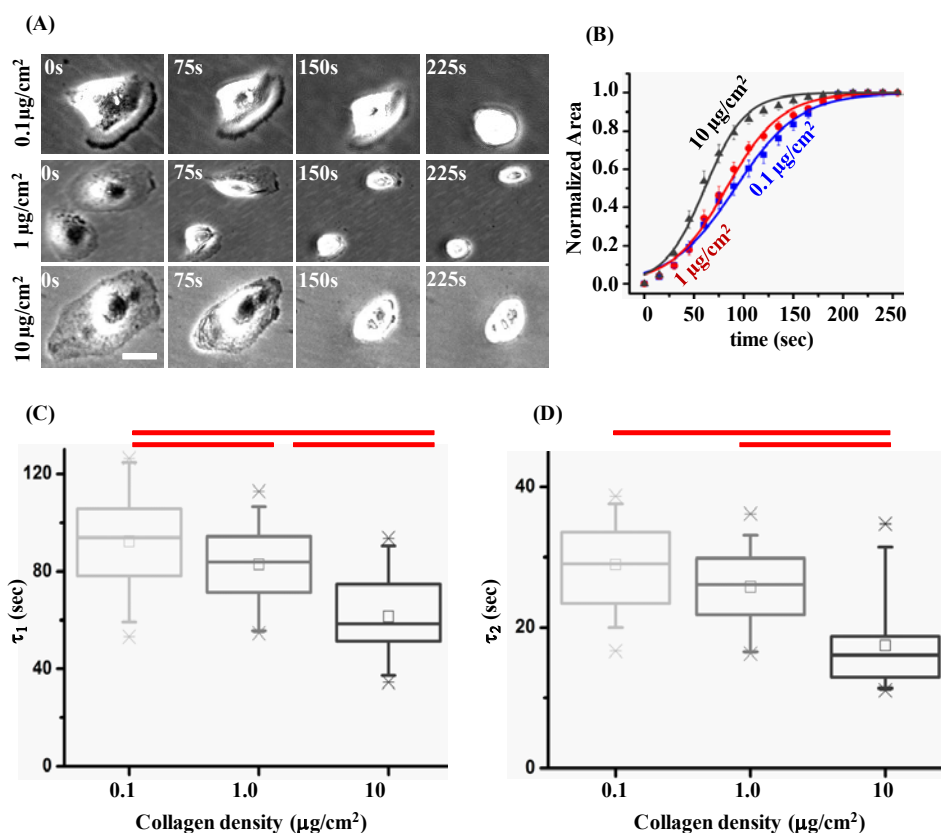


Figure 3: De-adhesion dynamics of MDA-MB-231 cells on collagen-coated surfaces at varying densities. (A) Upon incubation with trypsin, cells were imaged every 3 seconds till they rounded up but remained attached to the substrate. Representative images of cell rounding on various surfaces. Scale bar=50 µm. (B) De-adhesion of the cells were quantified by plotting normalized area as a function of time. Mean de-adhesion curves (points) at different densities reveal faster de-adhesion at higher densities. The lines denote fit of the experimental curves with Boltzmann equation. (C, D) Boltzmann fits to experimental curves yielded time constants τ_1 and τ_2 for each condition. Increase in collagen density led to reduction in both time constants. Bars indicate statistical significance ($p < 0.05$).

density surfaces exhibited higher number of invadopodia. Specifically, in comparison to ~2 invadopodia/cell observed on the lowest density surface, ~4 invadopodia/cell were observed on the intermediate density surface and ~8 invadopodia/cell were observed at the highest density (Figure 5B). Collectively, these results indicate that the enhanced degradation observed on higher density surfaces is orchestrated by the formation of more number of invadopodia on denser substrates.

Influence of cellular contractility on ECM degradation

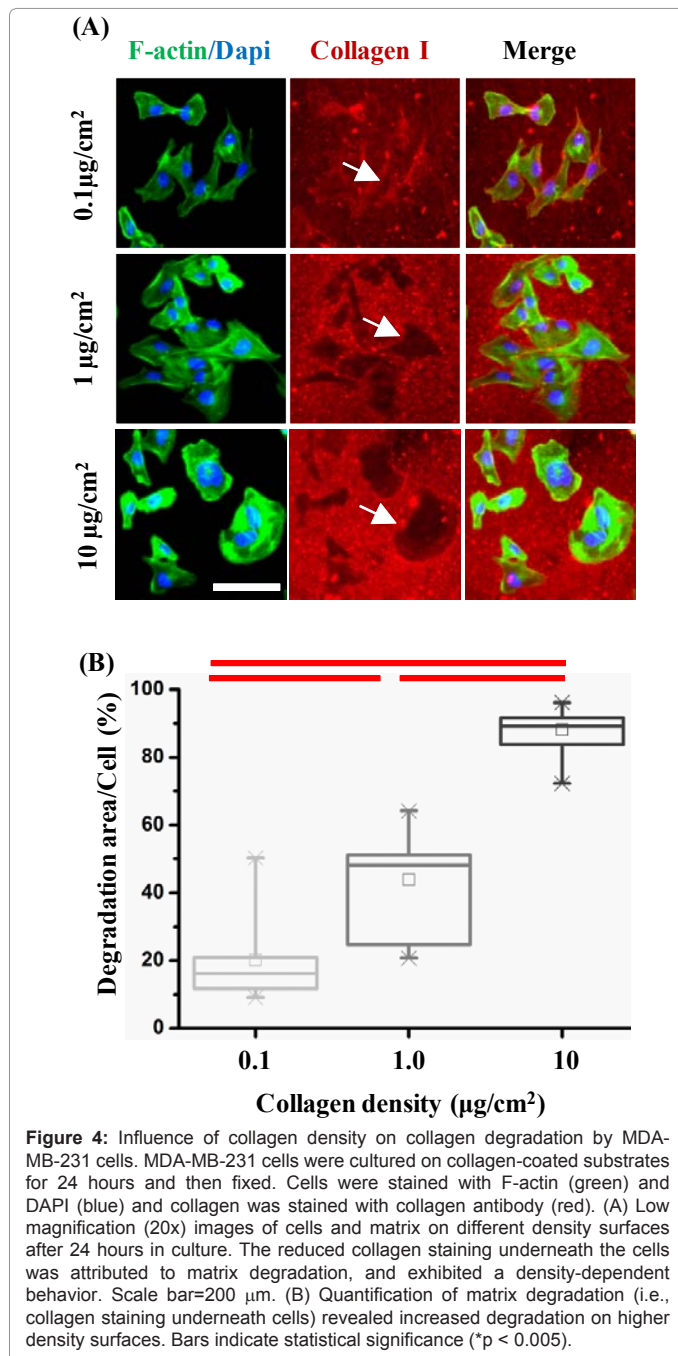
Thus far, our data suggests that higher ECM density is associated with stronger adhesions, enhanced cellular contractility and increased ECM degradation. Adherent cells are known to sense the physical properties of their underlying substrate using myosin-based contractile forces. Further, Weaver and coworkers had demonstrated the role of myosin II in the regulation of invadopodia activity. Therefore, it is possible that highest degradation on the 10 µg/cm² surfaces is attributed to the enhanced cellular contractility on these surfaces. To test this directly, cells were cultured on the 10 µg/cm² surfaces in the presence and absence of the well-known myosin-inhibiting drug blebbistatin. In addition, cells were also cultured in the presence of the broad-spectrum MMP inhibitor GM6001. A concentration of 5 µM was chosen for both the drugs to minimize drastic drug-induced changes in cell shape. First, de-adhesion experiments were conducted to assess the extent of suppression of contractility at the chosen drug

concentrations. Blebbistatin treatment led to statistically significant ~70% increase in both the time constants demonstrating the robust effect of blebbistatin in inhibiting contractility even at such a low concentration (Figure 6). Interestingly, de-adhesion was delayed even with GM6001 treatment, with a ~25% increase in τ_1 . However, τ_2 remained unaltered. Collectively, these results suggested that both blebbistatin and GM6001 suppressed cell contractility at the chosen concentration.

Given the reduction in cell contractility observed with both the drugs, we probed the extent of ECM degradation observed in drug-treated samples compared to untreated controls. Indeed, quantitative analysis of the degradation pattern at 24 hours visualized using collagen I antibody revealed negligible degradation in both blebbistatin-treated and GM6001-treated samples (Figures 7A and 7B). Furthermore, there was a significant reduction in the number of actin and cortactin-positive invadopodia (i.e., actin/cortactin co-localized dots) in the drug-treated cells (Figure 7C). In comparison to ~6 invadopodia/cell observed in untreated cells, ~4 invadopodia/cell was observed in GM6001-treated cells and ~1 invadopodia/cell observed in blebbistatin-treated cells (Figure 7D). Taken together, these results demonstrate the direct influence of contractility in modulating ECM degradation.

Contribution of MMPs to ECM degradation

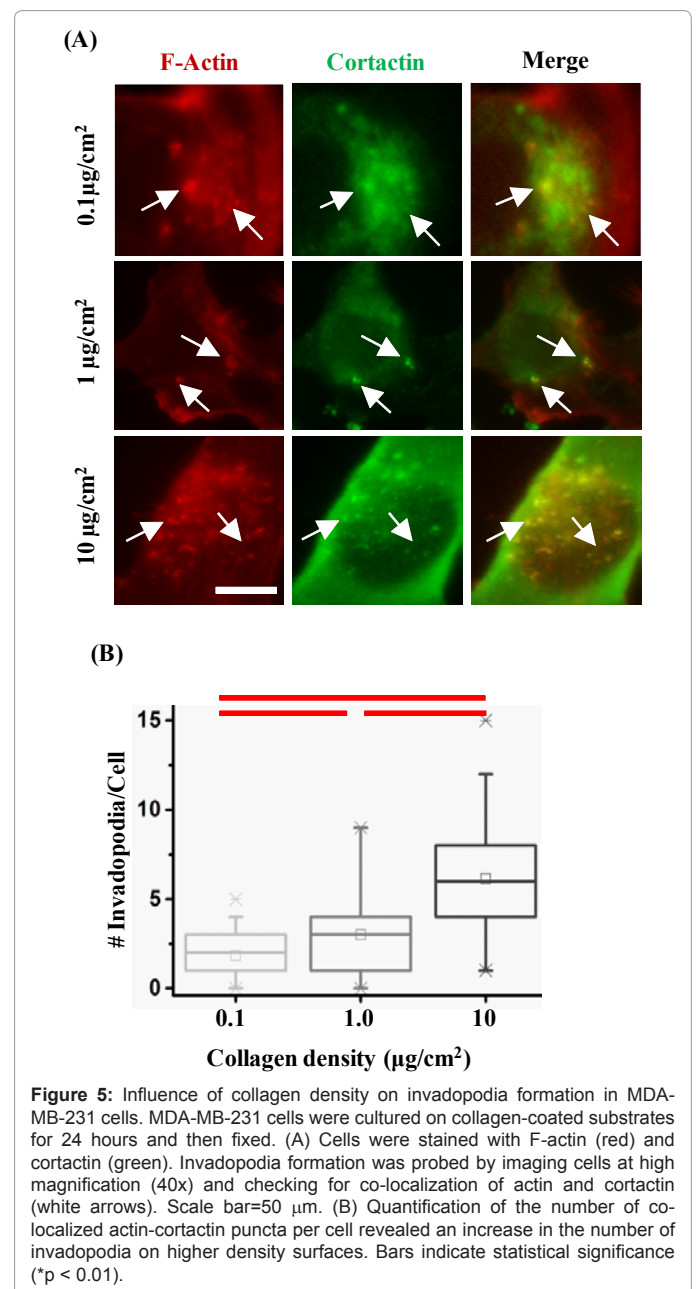
Though our results demonstrate the prominent role of contractility

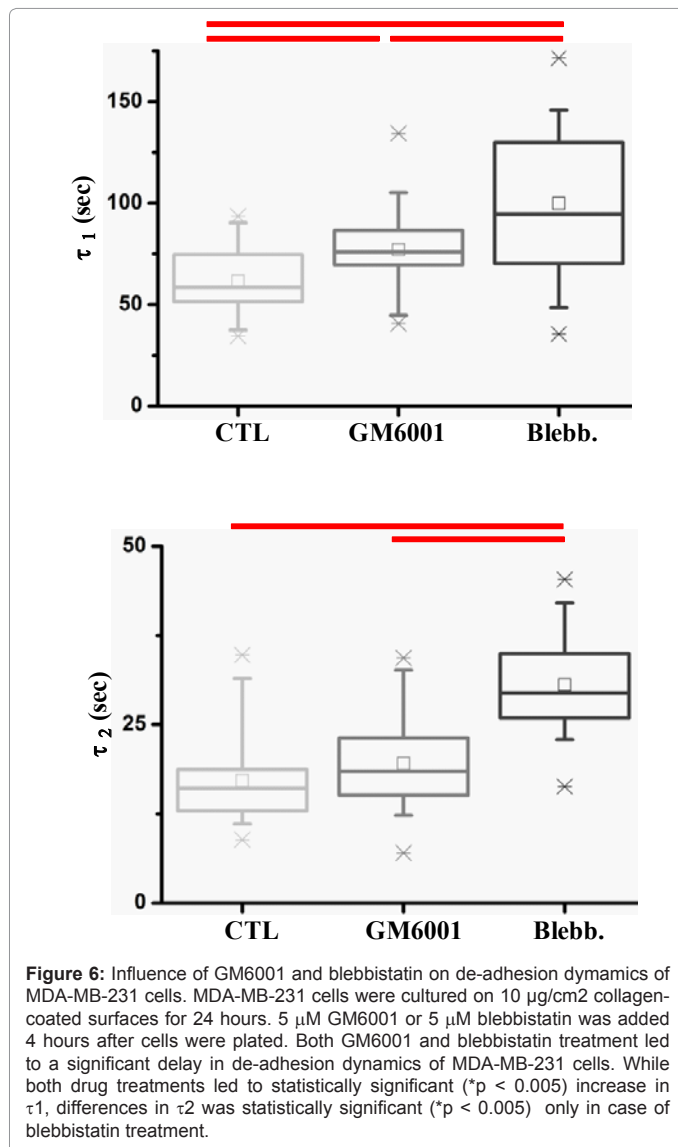


in modulating degradation, it remains unclear if reduced degradation in drug-treated cells was due to reduced expression of certain key degrading enzymes or reduced localization at invadopodia. It is well known that invadopodia are enriched in a range of metalloproteinases including MMP-2, MMP-9 and MT1-MMP (also referred to as MMP-14). While MT1-MMP is membrane-anchored, MMP-2 and MMP-9 are secreted. MMP-9 has been documented to actively degrade collagen I and III [31], and plays a distinct role in tumor angiogenesis. To test if ECM degradation was mediated by MMPs, ECM-density dependent activity of MMPs was checked using gelatin zymography. For doing this, equal number of cells was placed on the different collagen-coated surfaces and the supernatant was collected after 24 hours and processed for zymography (see methods). Interestingly, the activity of both MMP-

2 and MMP-9 exhibited a density-dependence with maximal activity observed on the 10 µg/cm² surfaces, with MMP-9 exhibiting a stronger density dependence compared to MMP-2 (Figure 8A).

Since cell contractility also increased with ligand density, therefore, to probe if MMP activity required cellular contractility, control, GM6001-treated and blebbistatin-treated cells were cultured on the highest 10 µg/cm² surfaces for 24 hours, and then processed for assessing the MMP activity levels (Figure 8B). In contrast to control cells, MMP activity as evaluated by gelatin degradation, was significantly reduced in both GM6001-treated and blebbistatin-treated cells. While densitometric analysis revealed a ~90% reduction in MMP-9 activity for both drug treatments, MMP-2 levels were relatively less sensitive to contractile inhibition at the drug dosage used, with ~65% reduction in blebbistatin-treated cells and ~35% reduction in GM6001-treated cells (Figure 8B).





Similar to the behavior of the secreted MMPs (MMP-2 and MMP-9), MT1-MMP which is membrane anchored, also exhibited a contractility-dependent behavior. Specifically, the activity of invadopodia measured from the co-localization of cortactin and MT1-MMP was found to decrease significantly both in GM6001-treated cells and in blebbistatin-treated cells (Figures 8C and 8D). Collectively, these results demonstrate that ECM degradation was mediated by MMPs in a contractility-dependent manner.

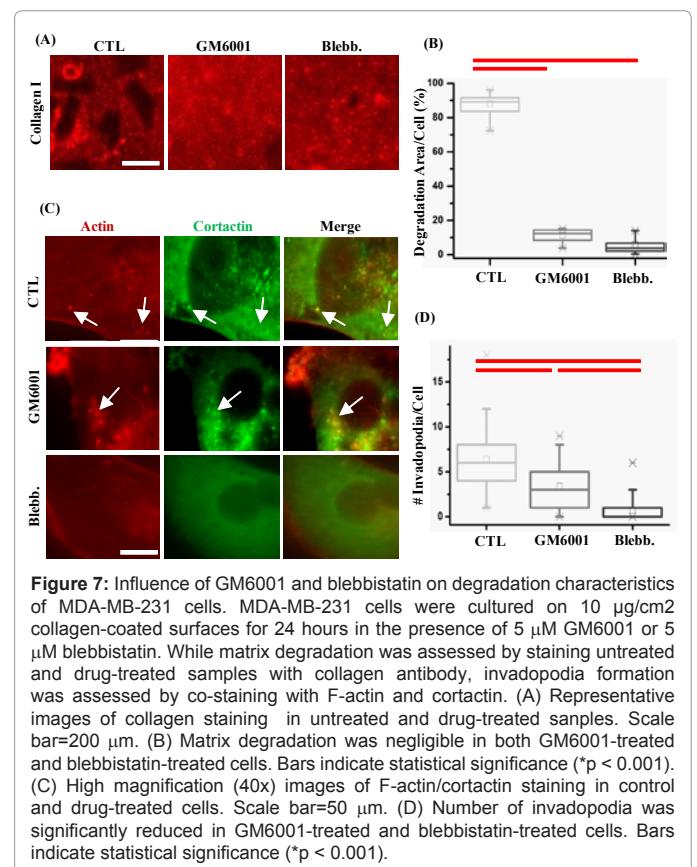
Discussion

In this study, we sought to determine the relationship between ECM density and the degradation characteristics of breast cancer cells. First, we have shown that ECM density promotes spreading of MDA-MB-231 cells in a density-dependent manner through the formation of stable focal adhesions. Second, using trypsin de-adhesion assay we have demonstrated that ECM density activates cell contractility. To our surprise, we found that cells exhibit stronger degradation on higher density surfaces through the formation of invadopodia. Degradation was suppressed upon treatment with either the non-muscle myosin inhibitor blebbistatin or the broad-spectrum MMP inhibitor GM6001,

both of which were found to inhibit cell contractility. Lastly, we have shown that degradation was mediated by MMP-2, MMP-9 and MT1-MMP in a contractility-dependent manner. Together, our results demonstrate that ECM density regulates ECM degradation through modulation of cell contractility.

Comparison of spreading and de-adhesion dynamics of breast cancer cells on collagen-coated surfaces illustrates the strong coupling between the two phenomena. At the 24 hour time point, cell spreading on the lowest coating density of 0.1 µg/cm² was nearly 3-fold compared to that on pluronic indicative of minimum deposition of serum proteins or ECM proteins secreted by cells themselves. Increase of coating density from 0.1 µg/cm² to 10 µg/cm² led to a nearly 100% increase in cell spreading area. Similar density-dependent spreading has been observed with various other cell types [5,8]. Higher cell spreading was associated with the formation of more number and larger-sized focal adhesions. This may be attributed to stronger integrin activation on higher density surfaces, with altered levels of phosphorylation of signaling proteins like Src and focal adhesion proteins like FAK and paxillin on higher density surfaces [10,32]. Faster de-adhesion observed with increase in ECM density suggests that increased contractility is associated with increased spreading, and has also been reported in fibroblasts and endothelial cells [6,33]. Similar ECM density-dependent de-adhesion response has also been observed on fibronectin-coated surfaces and in other cancer cell lines illustrating the generality of the findings [34,35].

Increased deposition of collagen I [36], LOX-mediated collagen crosslinking [4], and collagen fibril alignment are all known to promote cancer invasiveness [3,37] and have been implicated in the pathogenesis of breast, prostate and ovarian cancer [38]. Several studies have focused



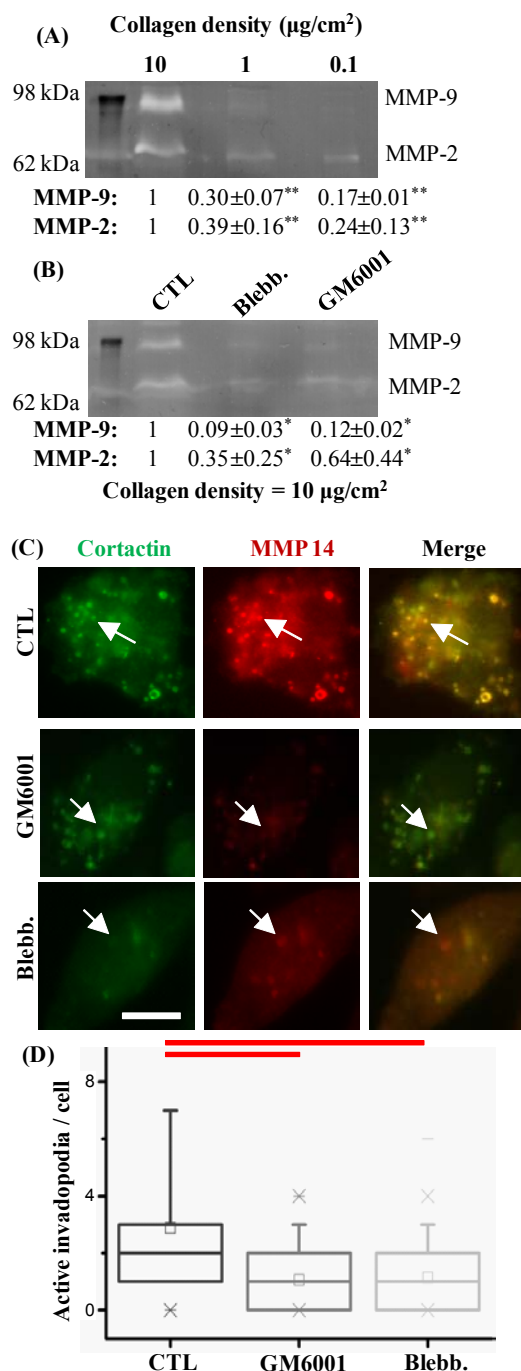


Figure 8: Contribution of MMPs to ECM degradation. MDA-MB-231 cells were cultured on collagen-coated substrates. After 24 hours, the supernatant was collected and the activity of MMPs evaluated using gelatin zymography. (A) Blots are representative of three independent experiments. Both MMP-2 and MMP-9 activity increased with increase in ligand density (** $p < 0.001$). (B) MDA-MB-231 cells were cultured on $10 \mu\text{g}/\text{cm}^2$ collagen-coated surfaces in the presence of $5 \mu\text{M}$ GM6001 or $5 \mu\text{M}$ blebbistatin. After 24 hours, the supernatant was collected and the activity of MMPs evaluated using gelatin zymography. The activity of both MMP-2 and MMP-9 were significantly reduced in drug-treated cells (* $p < 0.05$). (C) High magnification (40x) images of cortactin/MT1-MMP co-localization in control and drug-treated cells. Scale bar = $50 \mu\text{m}$. (D) Number of active invadopodia, i.e., number of co-localized cortactin/MT1-MMP dots, was significantly reduced in GM6001-treated and blebbistatin-treated cells. Bars indicate statistical significance (* $p < 0.001$).

on understanding how changes in ECM composition and physical properties regulate the behavior of normal and cancer cells. While ECM stiffness has been associated with increased cell proliferation, motility and degradation, ECM density has been associated with increased traction forces in metastatic cancer cells compared to their non-invasive counterparts [8]. Since we have observed differences in the extent of degradation on substrates of identical stiffness (i.e., glass) but varying ECM density, our results indicate that ECM density can regulate degradation independent of ECM stiffness. Moreover, this density-dependent degradation is closely tied to density-dependent increase in cellular contractility, as myosin inhibition significantly suppressed ECM degradation. While similar density-dependent degradation was also observed on gelatin-coated and fibronectin-coated substrates (Figures S1 and S2), it remains to be seen if this trend holds good for other ECM proteins like laminin and vitronectin.

Invadopodia are subcellular actin-rich protrusions used by cancer cells for degrading ECM using various degrading machinery including MMPs, ADAMs and cathepsins. The localization of multiple focal adhesion proteins at invadopodia have raised the possibility that invadopodia are adhesive structures, though this remains an open question. Further, it is unclear if there is any crosstalk between invadopodia and focal adhesions. Interestingly, in breast cancer cells, the FAK-Src complex was found to differentially regulate the balance between focal adhesions and invadopodia [39]. More recently, using live-cell imaging, Weaver and co-workers demonstrated that adhesion rings surround invadopodia immediately after their formation and contribute to invadopodia maturation [40]. However, no correlation was observed between the number and size of focal adhesions with invadopodia activity. In our studies, the prevalence of bigger focal adhesions and more number of invadopodia on higher density substrates raises the possibility of a coupling between these two structures, where stronger and stable adhesions lead to formation of more number of invadopodia and higher invadopodia activity, as measured using ECM degradation.

Since invadopodia arise from cell interactions with their surrounding matrix, therefore, physical properties of the matrix are likely to influence the formation and dynamics of invadopodia. Matrix dimensionality (i.e., organization), crosslinking, topography and rigidity have all been shown to play important roles in regulating cell behavior [4,11,41]. In a seminal work, Weaver and co-workers demonstrated the direct influence of ECM rigidity on invadopodia formation and activity, with phosphorylation levels of FAK and p130Cas found to localize at active invadopodia in a myosin-dependent manner [19]. In a follow up work, work from the same group demonstrated that optimal invadopodia activity was observed at 30 kPa [20]. Intriguingly, the study also found the existence of a second peak in invadopodia activity at 2 GPa . This is comparable to the stiffness of glass coverslips, substrates on which our studies were conducted. In combination with the above reports, our findings suggest that both ECM rigidity and ECM density influence invadopodia activity, and, on substrates of identical stiffness, ECM density may dictate the invasive response of cancer cells.

In our experiments, matrix degradation was mediated by MMP-2, MMP-9 and MT1-MMP, and required myosin activity. Though surprising, increasing evidence in different cell systems point to the close crosstalk between cell-matrix adhesion, cell generated forces and protease activity. In melanoma cells cultured on collagen-I, matrix degradation via MT1-MMP required a functional actomyosin network [42]. Disruption of actin network by cytochalasin D, or inhibition of myosin II activity by blebbistatin, suppressed cleavage of collagen fibers.

Further, the effects of blebbistatin on matrix degradation and inhibition of contractility required separate doses, with degradation abolished even at doses of 1 μ M, and contractility inhibition requiring higher doses. However, the drug-induced differences were not associated with any trafficking defects, as cell surface expression of MT1-MMP remained unaltered under the drug treatments. In tenocytes, the expression of MMP-1 was found to depend on cytoskeletal tension [43]. While the above results indicate a direct dependency of MMP expression on contractility, the recovery of contractile function by inhibition of MMP-2 in myocardial ischemia suggests a more complicated relationship [44]. Indeed, the reduction in cell contractility upon treatment with GM6001, observed in our studies, indicates a bi-directional relationship between MMPs and myosin II. Similar results have been reported in fibroblasts where GM6001 treatment was found to inhibit collagen matrix contraction [45]. Collectively, these results indicate that cell generated traction forces and MMPs regulate each other for efficient proteolysis.

In summary, our results demonstrate an intimate relationship between ECM density and extracellular proteolysis in invasive breast cancer cells modulated by cell contractility. Future work will be focused on probing the mechanism of the bi-directional crosstalk between contractility and MMPs uncovered in this work.

Acknowledgement

A. D. was supported by a fellowship from DBT. S. S. gratefully acknowledges financial support from BRNS (2011/20/37B/09/BRNS) and IIT Bombay (Healthcare Grant) for carrying out this work.

References

1. Kalluri R (2003) Basement membranes: structure, assembly and role in tumour angiogenesis. *Nat Rev Cancer* 3: 422-433.
2. Provenzano PP (2006) Collagen reorganization at the tumor-stromal interface facilitates local invasion. *BMC Med* 4: 38.
3. Provenzano PP, Inman DR, Eliceiri KW, Knittel JG, Yan L, et al. (2008) Collagen density promotes mammary tumor initiation and progression. *BMC Med* 6: 11.
4. Levental KR, Yu H, Kass L, Lakins JN, Egeblad M, et al. (2009) Matrix crosslinking forces tumor progression by enhancing integrin signaling. *Cell* 139: 891-906.
5. Engler A, Bacakova L, Newman C, Hategan A, Griffin M, et al. (2004) Substrate compliance versus ligand density in cell on gel responses. *Biophys J* 86: 617-628.
6. Gaudet C, Marganski WA, Kim S, Brown CT, Gunderia V, et al. (2003) Influence of type I collagen surface density on fibroblast spreading, motility, and contractility. *Biophys J* 85: 3329-3335.
7. Peyton SR, Putnam AJ (2005) Extracellular matrix rigidity governs smooth muscle cell motility in a biphasic fashion. *J Cell Physiol* 204: 198-209.
8. Kraning-Rush CM, Califano JP, Reinhart-King CA (2012) Cellular traction stresses increase with increasing metastatic potential. *PLoS One* 7: e32572.
9. Ulrich TA, de Juan Pardo EM, Kumar S (2009) The mechanical rigidity of the extracellular matrix regulates the structure, motility, and proliferation of glioma cells. *Cancer Res* 69: 4167-4174.
10. Paszek MJ, Zahir N, Johnson KR, Lakins JN, Rozenberg GI, et al. (2005) Tensional homeostasis and the malignant phenotype. *Cancer Cell* 8: 241-254.
11. Doyle AD, Wang FW, Matsumoto K, Yamada KM (2009) One-dimensional topography underlies three-dimensional fibrillar cell migration. *J Cell Biol* 184: 481-490.
12. Kraning-Rush CM, Carey SP, Lampi MC, Reinhart-King CA (2013) Microfabricated collagen tracks facilitate single cell metastatic invasion in 3D. *Integr Biol (Camb)* 5: 606-616.
13. Buccione R, Orth JD, McNiven MA (2004) Foot and mouth: podosomes, invadopodia and circular dorsal ruffles. *Nat Rev Mol Cell Biol* 5: 647-657.
14. Gimona M, Buccione R, Courtneidge SA, Linder S (2008) Assembly and biological role of podosomes and invadopodia. *Curr Opin Cell Biol* 20: 235-241.
15. Linder S (2007) The matrix corroded: podosomes and invadopodia in extracellular matrix degradation. *Trends Cell Biol* 17: 107-117.
16. Linder S (2009) Invadosomes at a glance. *J Cell Sci* 122: 3009-3013.
17. Artym VV, Zhang Y, Seillier-Moisewitsch F, Yamada KM, Mueller SC (2006) Dynamic interactions of cortactin and membrane type 1 matrix metalloproteinase at invadopodia: defining the stages of invadopodia formation and function. *Cancer Res* 66: 3034-3043.
18. Schoumacher M, Goldman RD, Louvard D, Vignjevic DM (2010) Actin, microtubules, and vimentin intermediate filaments cooperate for elongation of invadopodia. *J Cell Biol* 189: 541-556.
19. Alexander NR, Branch KM, Parekh A, Clark ES, Iwueke IC, et al. (2008) Extracellular matrix rigidity promotes invadopodia activity. *Curr Biol* 18: 1295-1299.
20. Parekh A, Ruppender NS, Branch KM, Sewell-Loftin MK, Lin J, et al. (2011) Sensing and modulation of invadopodia across a wide range of rigidities. *Biophys J* 100: 573-582.
21. Enderling H, Alexander NR, Clark ES, Branch KM, Estrada L, et al. (2008) Dependence of invadopodia function on collagen fiber spacing and cross-linking: computational modeling and experimental evidence. *Biophys J* 95: 2203-2218.
22. Sen S, Ng WP, Kumar S (2012) Contributions of talin-1 to glioma cell-matrix tensional homeostasis. *J R Soc Interface* 9: 1311-1317.
23. Anderl J, Ma J, Armstrong L (2012) Fluorescent Gelatin Degradation Assays for Investigating Invadopodia Formation. *Nature Methods* 121007: 1-5.
24. Martin KH, Hayes KE, Walk EL, Ammer AG, Markwell SM, et al. (2012) Quantitative measurement of invadopodia-mediated extracellular matrix proteolysis in single and multicellular contexts. *J Vis Exp* : e4119.
25. Pignatelli J, LaLonde SE, LaLonde DP, Clarke D, Turner CE (2012) Actopaxin (β -parvin) phosphorylation is required for matrix degradation and cancer cell invasion. *J Biol Chem* 287: 37309-37320.
26. Lu P, Weaver VM, Werb Z (2012) The extracellular matrix: a dynamic niche in cancer progression. *J Cell Biol* 196: 395-406.
27. Sen S, Kumar S (2009) Cell-Matrix De-Adhesion Dynamics Reflect Contractile Mechanics. *Cell Mol Bioeng* 2: 218-230.
28. Egeblad M, Werb Z (2002) New functions for the matrix metalloproteinases in cancer progression. *Nat Rev Cancer* 2: 161-174.
29. Linder S, Wiesner C, Himmel M (2011) Degrading devices: invadosomes in proteolytic cell invasion. *Annu Rev Cell Dev Biol* 27: 185-211.
30. Linder S (2009) Invadosomes at a glance. *J Cell Sci* 122: 3009-3013.
31. Bigg HF, Rowan AD, Barker MD, Cawston TE (2007) Activity of matrix metalloproteinase-9 against native collagen types I and III. *FEBS J* 274: 1246-1255.
32. Pelham RJ Jr, Wang YI (1997) Cell locomotion and focal adhesions are regulated by substrate flexibility. *Proc Natl Acad Sci U S A* 94: 13661-13665.
33. Califano JP, Reinhart-King CA (2010) Substrate Stiffness and Cell Area Predict Cellular Traction Stresses in Single Cells and Cells in Contact. *Cell Mol Bioeng* 3: 68-75.
34. Kapoor A, Sen S (2012) Synergistic modulation of cellular contractility by mixed extracellular matrices. *Int J Cell Biol* 2012: 471591.
35. Sen S, Ng WP, Kumar S (2011) Contractility dominates adhesive ligand density in regulating cellular de-adhesion and retraction kinetics. *Ann Biomed Eng* 39: 1163-1173.
36. Ursin G, Hovanessian-Larsen L, Parisky YR, Pike MC, Wu AH (2005) Greatly increased occurrence of breast cancers in areas of mammographically dense tissue. *Breast Cancer Res* 7: R605-608.
37. Yang N, Mosher R, Seo S, Beebe D, Friedl A (2011) Syndecan-1 in breast cancer stroma fibroblasts regulates extracellular matrix fiber organization and carcinoma cell motility. *Am J Pathol* 178: 325-335.
38. Nadiarnykh O, LaComb RB, Brewer MA, Campagnola PJ (2010) Alterations

- of the extracellular matrix in ovarian cancer studied by Second Harmonic Generation imaging microscopy. *BMC Cancer* 10: 94.
39. Chan KT, Cortesio CL, Huttenlocher A (2009) FAK alters invadopodia and focal adhesion composition and dynamics to regulate breast cancer invasion. *J Cell Biol* 185: 357-370.
40. Branch KM, Hoshino D, Weaver AM (2012) Adhesion rings surround invadopodia and promote maturation. *Biol Open* 1: 711-722.
41. Geblinger D, Addadi L, Geiger B (2010) Nano-topography sensing by osteoclasts. *J Cell Sci* 123: 1503-1510.
42. Kirmse R, Otto H, Ludwig T (2011) Interdependency of cell adhesion, force generation and extracellular proteolysis in matrix remodeling. *J Cell Sci* 124: 1857-1866.
43. Maeda E, Sugimoto M, Ohashi T (2013) Cytoskeletal tension modulates MMP-1 gene expression from tenocytes on micropillar substrates. *J Biomech* 46: 991-997.
44. Ali MA, Stepanko A, Fan X, Holt A, Schulz R (2012) Calpain inhibitors exhibit matrix metalloproteinase-2 inhibitory activity. *Biochem Biophys Res Commun* 423: 1-5.
45. Martin-Martin B, Tovell V, Dahlmann-Noor AH, Khaw PT, Bailly M (2011) The effect of MMP inhibitor GM6001 on early fibroblast-mediated collagen matrix contraction is correlated to a decrease in cell protrusive activity. *Eur J Cell Biol* 90: 26-36.

This article was originally published in a special issue, [Cell-Extracellular Matrix Interactions in Carcinogenesis](#) handled by Editor(s). Dr. Claudio Luparello, University of Palermo, Italy